Environment Protection Engineering

Vol. 52 2026 No. 2

DOI: 10.37190/epe/218300

XIAOFENG ZHANG (ORCID: 0009-0001-6906-6599)[1]
SHIHANG ZHENG (ORCID: 0009-0006-0363-0157)[1]
RUI ZHENG (ORCID: 0009-0001-3484-1639)[1]
XIAOHAN WEI (ORCID: 0009-0003-9054-2638)[1]
ZHENGCHENG WEN (ORCID: 0000-0001-9224-2610)[1]

DYNAMICS SIMULATION OF MICROWAVE DISCHARGE FOR TOLUENE REMOVAL BY COUPLING PLASMA FIELD AND CHEMICAL REACTION MECHANISM

The microwave discharge method is recognized as a highly promising technology for volatile organic compounds (VOC) treatment, owing to its advantages of high removal efficiency, high reaction rates, and minimal secondary pollution. In this study, numerical simulations of microwave discharge cracking for toluene removal were conducted using COMSOL Multiphysics software coupled with plasma physical fields and Fluent software coupled with chemical reaction mechanisms. The optimal operational parameters were determined through model optimization, aiming to provide practical numerical references for industrial applications. Under microwave irradiation, the production of •OH radicals and toluene removal efficiency were investigated across varying microwave powers, temperatures, flue gas inlet rates, gas compositions, and other operational conditions. Principal influencing factors were analyzed, revealing that microwave power and temperature predominantly influence removal efficiency, with higher values resulting in significantly improved efficiency. Factors such as flue gas inlet rate, moisture concentration, and oxygen content also exert notable effects on toluene removal efficiency. This study identified that at 523 K, with 5% oxygen and moisture content in the flue gas, an inlet rate of 3 m/s, an initial toluene concentration of 1 ppm, and a microwave power of 3000 W in the ion reactor, optimal conditions were achieved, achieving a toluene removal efficiency of 97.83%. These findings are crucial for advancing the engineering applications of toluene removal technologies.

I. INTRODUCTION

Volatile organic compounds (VOCs) present a significant threat to human health and the environment, with documented detrimental effects on respiratory and visual systems [1].

[1]Institute of Energy, Hangzhou Dianzi University, Hangzhou, China, 310018, corresponding author Z. Wen, email address: wenzc@hdu.edu.cn

Excessive VOC emissions contribute to urban haze and serious environmental pollution [2], underscoring the urgent need for cost-effective VOCs removal methods. Current technologies for VOC treatment and control encompass physical adsorption [3], oxidation processes [4], plasma methods [5, 6], and catalytic combustion [7]. Among these, the microwave plasma method stands out as a promising VOC treatment technology due to its high removal efficiency, rapid reaction rates, and minimal secondary pollution.

The microwave plasma method achieves VOC oxidation and removal by generating potent oxidizing substances such as •OH/•O radicals through processes like pulsed corona discharge and metal dielectric discharge in air. These reactive species then oxidize VOCs into environmentally benign products such as H_2O, CO_2, and H_2. Microwave power and the concentration of •OH radicals significantly influence VOC removal [8, 9]. Previous studies have confirmed the technical feasibility of microwave metal discharge cracking of VOCs [8] and demonstrated the effective removal of VOCs such as alkanes, benzene, and toluene by •OH radicals [10, 11].

The adoption of multiphysics simulation software, such as COMSOL Multiphysics, and Computational Fluid Dynamics (CFD) simulation tools like Fluent [12, 13] has significantly reduced research costs in this field, thereby shortening the development cycle of removal technologies. For instance, Mousavi et al. [14] employed CFD to simulate a laboratory-scale biomass boiler, identifying different pathways of NO_x formation and their role and contribution.

Previous studies have shown that microwave irradiation is beneficial for the removal of VOCs. Feng et al. [15] studied the effect of microwave-induced metal discharge on the removal of VOCs represented by acetone. The results indicate that when acetone with a concentration of 200 ppm is in a microwave environment, the removal efficiency of acetone is between 40% and 60%. At the microwave power of 900 W, the removal efficiency can reach up to 65%. In 2022, Wang et al. [16] investigated microwave-enhanced VOCs catalytic degradation numerically and experimentally using a novel double ridge field compression cavity. They conducted degradation experiments on ethanol, benzene, and acetone under microwave conditions, and numerically simulated the electric field and temperature field using COMSOL Multiphysics software. The simulation results of the electric field distribution and temperature distribution in the cavity present a similar trend to the experimental results. Li et al. [17] achieved effective removal of toluene and acetone by Cu-Mn-CeO_x modified substrates at a microwave power of 250 W.

Microwave plasma methods induce discharge in air, generating highly reactive electrons and radicals, leading to various chemical reactions [18]. The reaction mechanism of •OH radicals acting on toluene involves the activation of methyl groups [19], with a preference for targeting specific binding sites and carbon positions, ultimately leading to the breakdown of the benzene ring. This study utilizes the finite element method to calculate microwave plasma physical fields and employs a coupled CFD method to investigate the efficiency of microwave discharge-induced plasma removal of VOCs, using toluene as a case study. The study explores the reaction pattern of toluene removal by •OH radicals

under microwave irradiation and analyzes the key factors affecting toluene removal efficiency. The optimal reaction conditions for toluene removal are determined to provide reference and support for practical industrial production and application.

2. CALCULATION METHODS AND SIMULATION DETAILS

Microwave plasma reaction chamber. Initially, the flue gas duct and microwave generator were modeled within COMSOL, as shown in Fig. 1a, to facilitate the simulation and calculation of microwave plasma generation within the duct. A simplified 2D simulation was conducted to analyze the microwave plasma physics field. The 2D mesh was constructed using a combination of triangular and quadrilateral elements, effectively discretizing the region (Fig. 1b). The average cell mass of the resulting grid was determined to be 0.722.

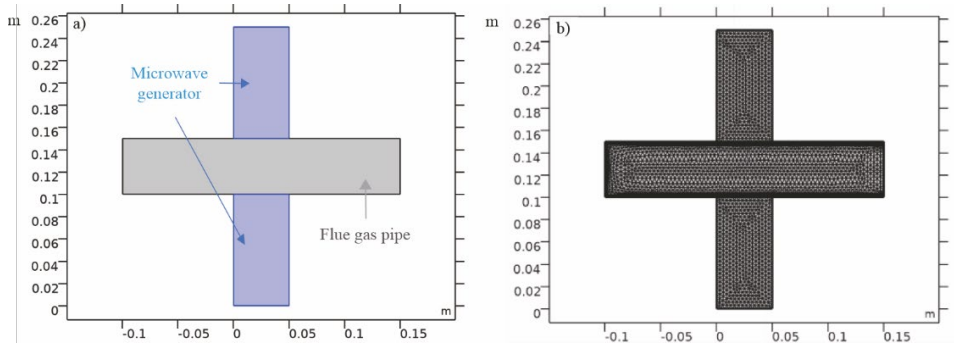

Fig. 1. Schematic diagrams of flue gas duct and microwave generator:
a) model schematic, b) mesh schematic

Electronic reaction chamber. The Monte Carlo simulation [20] was employed in MATLAB to construct an electron reaction chamber replicating the structure of the microwave plasma reaction chamber described previously. This simulation aimed to ionize the air within the chamber to generate •OH radicals. The chamber was designed to facilitate electron collision reactions and charge transfer reactions, with the electron reaction chamber positioned centrally within the flue gas duct. This location was chosen because the microwave discharge reactions are primarily concentrated in this region, which is subject to microwave irradiation. To simplify calculations, the electron density within the duct model was averaged, assuming a uniform distribution of the reactor components.

Electron reaction chamber setup. A 2D electron reactor space measuring 34×17 cm was configured, matching the size of the microwave reactor (Fig. 2). The electron density distribution within this reactor was derived from COMSOL simulations. The generation

of ·OH radicals through ionization in the microwave reaction chamber was simulated with a time span of 1 microsecond.

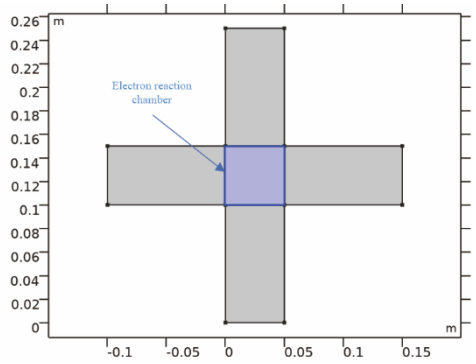

Fig. 2. Schematic diagram of the electronic reaction chamber

The primary components involved in the simulation were H_2O, O_2, and electrons. These components were used to model electron collision and charge transfer reactions leading to OH radical formation. The model included only O_2 and H_2O electrodes, while trace substances were omitted. The major source of ·OH radicals was modeled as involving only O_2 with H_2O electrodes. The initial average electron density and the conditions for each component in the reactor were set. The ODES solver was utilized for solving rigid ordinary differential equations involving a system of multiple interacting sub-processes with significant disparities in the rates of change.

Flue gas duct system. Subsequently, the analytical dispersion of VOCs (specifically, toluene) within the duct model was simulated using Fluent to determine the toluene removal efficiency (Fig. 3). The integrity of the model and its meshing are pivotal, as they directly impact the precision and computational efficiency of the simulations.

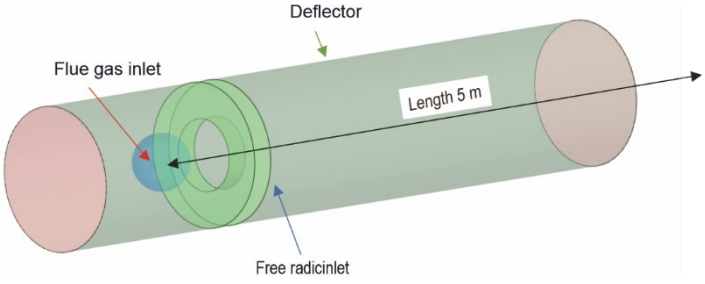

Fig. 3. Schematic diagram of the overall model of the flue gas duct

The flue gas duct was symmetrically divided into four equal segments along its longitudinal axis. By utilizing a quarter of the simplified duct model, the distribution and removal of VOC-containing gases were analyzed, thereby enhancing both the speed and

accuracy of the model's calculations (Fig. 4a). The duct's profile was designed to maintain symmetry, ensuring that it did not compromise the overall simulation results.

The mesh generation for the model was performed using ANSYS-Meshing, as shown in Fig. 4b. The process involved drawing a quadrilateral mesh and subsequently encrypting and flattening specific areas to improve mesh quality and enhance the efficiency and accuracy of the iterative process. The quality of the mesh is a critical factor affecting the speed and accuracy of Fluent computations, making it essential to inspect the mesh quality post-creation.

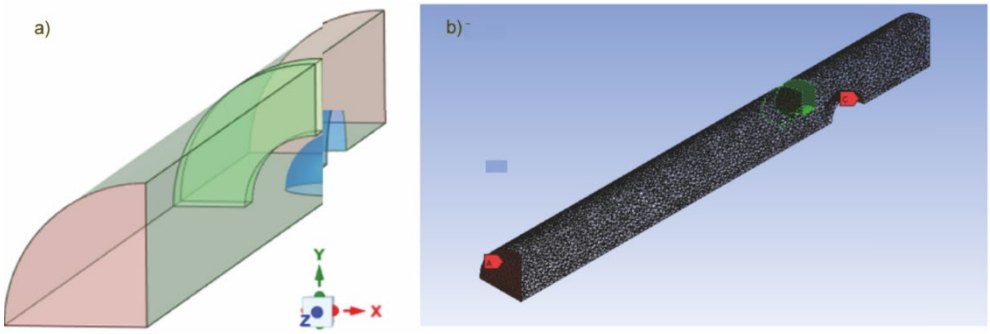

Fig. 4. Schematic diagram of 1/4 model of flue gas duct: a) 1/4 model schematic, b) 1/4 mesh schematic

ANSYS-Meshing was used to inspect the mesh. The Jacobian ratio, which is the ratio of the minimum to the maximum Jacobian determinant of the mesh's tetrahedral elements, serves as an indicator of mesh quality. A higher ratio closer to 1 signifies a better mesh quality. The Jacobian ratio was calculated and used as a metric to assess the degree of mesh distortion. The model's mesh was evaluated, with a mesh mass of approximately 0.275 at the smallest point, 0.998 at the largest point, and over 80% of the meshes having a mass greater than 0.82, with an average mass of 0.832. The mesh quality generally meets the requirements of this study, ensuring the convergence of the computational simulation and the acquisition of accurate simulation results.

Fluent solver setup. To simulate the distribution and degradation of gaseous pollutants within the duct over a 100-s period, the FLUENT calculation model was employed as a transient model with 500 time steps, each lasting 0.01 s. To ensure convergence at each step, the maximum number of iterations for each time step was selected. The influence of gravitational acceleration was disregarded, and considering the involvement of chemical reactions, the energy equation was taken into account. A possible choice for the turbulence model is the k-ε model. Its advantage over the standard k-ε model lies in its ability to maintain consistency with the Reynolds stress of actual turbulence and to more accurately simulate the diffusion velocity of the planar jet. The component transport model was chosen and linked to the CHEMKIN reaction mechanism and thermodynamic documents [19]. The finite-rate model (finite-rate/no turbulence-chemistry interaction, TCI) was

adopted due to the involvement of chemical reactions between components, with volume reaction and inlet diffusion between components being considered. The jet inlet and exhaust gas inlet were designated as velocity inlets, the pipeline outlet as a pressure outlet, the pipeline wall as a non-slip wall, and the interior as a symmetry plane. Standard initialization and all-zone selection were utilized, and the corresponding components and initial temperature were set accordingly.

Observation surface. An observation surface was positioned along the height of the pipeline, with cross sections for monitoring toluene concentration and surface standard deviation set at 1-meter intervals. Data were recorded every 200 time steps. This observation surface facilitated the monitoring of waste gas degradation efficiency (E_r) and uniformity as the distance increased.

$$E_r = \left(1 - \frac{C_{\text{out}}}{C_{\text{in}}}\right) \times 100\%$$

where C_{in} and C_{out} are the concentrations of toluene at the inlet and outlet of flue gas, respectively.

3. RESULT AND DISCUSSION

3.1. DISTRIBUTION OF •OH RADICALS IN GASEOUS POLLUTANTS

Initially, the electron distribution within the reactor under microwave irradiation was simulated based on reactions involving electron collision and charge transfer to generate •OH radicals. The microwave power used was set at 30 W. The gas composition within the reactor consisted of 90% nitrogen, 5% oxygen, and 5% water by molar fraction. The electron distribution in the reactor was computed at a time step of 0.01 s. Figure 5a illustrates that the electron distribution in the reactor was most uniform in the central region under microwave irradiation. In this central area, the electron density measured 1.15×10^{17}, closely approaching the ideal distribution of 7×10^{16} m^{-3} [21]. Given the concentration of electrons in this central zone, averaging was applied to simplify subsequent calculations. Figure 5b depicts the temporal evolution of electron density in the central region of the microwave reactor. Initially, the density decreased from 10^{17} m^{-3} to 6×10^{18} m^{-3} within the first 0.001 s. Subsequently, the electron density gradually increased, stabilizing around 1.15×10^{17} m^{-3} over subsequent time intervals. This behavior reflects a balance between electron generation and consumption rates, where initial electron generation rates were lower than consumption rates, leading to a gradual increase in density until equilibrium was achieved and the density reached saturation.

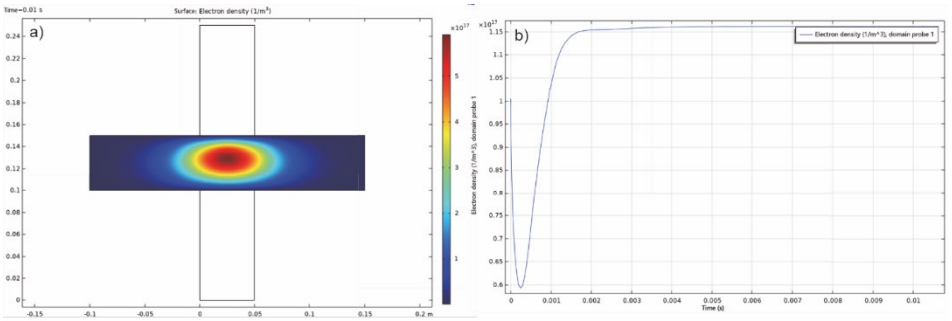

Fig. 5. 30 W microwave power: a) electron density, b) electron density versus time

We conducted simulations and analyses on the generation of •OH radicals within the reactor using electron collision and charge transfer reactions. The average electron density within the simulated reactor, determined in the preceding step, was 1.15×10^{17} m^{-3}. The gas composition within the reactor consisted of 90% nitrogen, 5% oxygen, and 5% water by molar fraction.

The electron collision reaction involves the production of primary radicals such as •O and •OH, as well as excited state molecules, through collisions between electrons and gas molecules at energies exceeding the ionization or dissociation thresholds of the gas molecules [22]. The rate constant for electron collision reactions can be determined using the following equation [23]:

$$\beta = \alpha \exp\left(-\frac{\beta}{E\left(N_T\right)^{-1}}\right)$$

where α depends on reactor and electrode geometry, cm^3/(molecule·s), β depends on ionization energy, Td (Townsend, 1 Td = 10^{-17} V·cm^2/molecule), cf. Table 1. N_T is the total gas density, molecules/cm^3, E is the electric field strength, V/cm, here E = 40 kV/cm.

Table 1

Electron collision reactor correlation coefficients

Symbol of the ate constant	α [cm^3/(molecule·s)]	β [Td]
$k_{e1}(O_2–O)$	1.3×10^{-8}	309
$k_{e2}(O_2–O1D)$	1×10^{-8}	338
$k_{e3}(H_2O)$	2×10^{-11}	322

The total gas density was calculated by incorporating the mixed air density into the aforementioned equation. The electron density distribution was modeled uniformly within the reactor through computational analysis with COMSOL. The densities of pertinent gas

components were predefined, and the resulting data were derived from solving a stiff ordinary differential equation (ode15s) within a time frame of 1 ms. Electronic collision reactions are given in Table 2.

Table 2

Electron collision reactions

Reaction	Rate constant [cm^3/(molecule·s)]
$e + O_2 = {}^{\bullet}O + {}^{\bullet}O + e$	$k_{c1} = 1.64132\times10^{-9}$
$e + O_2 = {}^{\bullet}O + O(1D) + e$	$k_{c2} = 1.0396810^{-9}$
$e + H_2O = {}^{\bullet}OH + {}^{\bullet}H + e$	$k_{c3} = 2.3145610^{-12}$

The production of the excited state atom O(1D) through electron collision reactions is a significant mechanism for generating primary radicals ·O and ·OH, in conjunction with charge transfer reactions involving the gas molecules at the electrode [22]. The primary source of ·OH generation is attributed to charge transfer reactions, given the comparatively lower yield of ·OH from electron collision reactions. As the reaction model for the electrode comprises only O_2 and H_2O, the charge transfer reactions are given in Table 3.

Table 3

Charge transfer reactions

Reaction	Rate constant [cm^3/(molecule·s)]
$O(1D) + H_2O = {}^{\bullet}OH + {}^{\bullet}OH$	$k_{e1} = 2.2\times10^{-10}$
$O(1D) + H_2O = {}^{\bullet}O + H_2O$	$k_{e2} = 1.2\times10^{-10}$
$O(1D) + O_2 = {}^{\bullet}O + O_2$	$k_{e3} = 3.8\times10^{-11}$

The electron density distribution within the reactor was modeled uniformly through computational analysis in COMSOL. The densities of the pertinent gas components were established, and the data were computed by solving a rigid ordinary differential equation (ode15s) over a time interval of 1 microsecond.

The radicals ·OH and ·O were generated via electron collision and charge transfer reactions as follows: the inlet flow rate of the radical was 2.91×10^{-8} m/s. The yield of ·OH radicals was 1.99×10^{17} molecules/s, with a corresponding molar fraction of 12.68% in the gas mixture. The yield of ·O radicals was 1.37×10^{18} molecules per second, accounting for a molar fraction of 87.32% in the gas components.

The distribution of pollutants was investigated through simulation calculations. The simulation conditions included a flue gas inlet velocity of 3 m/s, a temperature of 473 K, and a composition of 89.999% nitrogen by mole fraction, 5% of oxygen, 5% of water vapor, and 0.001% (10 ppm) of toluene. The flow velocity at radical inlet was 2.91×10^{-8} m/s and temperature 473 K, with an input gas fraction consisting of 87% oxygen and 13%

•OH radicals by mole fraction. Toluene concentrations across the cross-section were monitored at 1 m intervals, with standard deviations recorded.

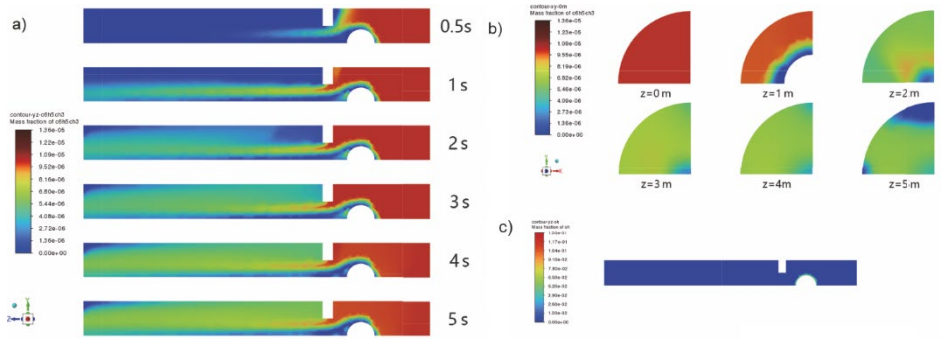

Fig. 6. Toluene concentration distribution in the pipe profile and its cross-section:
a) over time in the pipe profile, b) in the pipe cross-section after 5 s,
c) •OH radical distribution and concentration in the pipe profile after 5 s

Figure 6a illustrates that the gas distribution within the pipe stabilizes after approximately 5 s of simulation time, with toluene concentrations showing minimal change over time. The removal efficiency of toluene by •OH radicals under these conditions was assessed by monitoring the average toluene concentrations across the pipeline cross-section. In Figure 6b, the color intensity of the cloud plots corresponds to the molar concentration of toluene gas, with red indicating higher concentrations and blue indicating lower concentrations. It is observed that toluene concentrations decrease with increasing distance from 0 to 2 m. Beyond 2 m, the toluene concentration distribution remains uniform due to the presence of a deflector. In the 2–5 m interval, the distribution is also uniform with increasing distance, influenced by the deflector plate. Figure 6c reveals that •OH radicals are uniformly produced from the walls of the ion reaction chamber.

3.2. FACTORS AFFECTING THE EFFICIENCY OF TOLUENE REMOVAL

Building upon the aforementioned preliminary findings, the simulation of toluene removal under various operational conditions was conducted. The study investigated the generation of •OH radicals and the effectiveness of toluene removal by •OH radicals under microwave irradiation across different microwave power levels, temperatures, moisture concentrations, oxygen concentrations, flue gas inlet velocities, and toluene concentrations. The research aimed to identify the optimal operational parameters for •OH radical generation to facilitate toluene removal under microwave irradiation.

The inlet temperatures for both free radicals and flue gas were set at 473 K, with a flue gas inlet velocity of 3 m/s. The gas composition was adjusted using N_2 as the equilibrium gas. The ratio of •OH to C_7H_8 concentrations was controlled by varying the microwave reactor power. The impact of this ratio on pollutant removal efficiency and uniformity

was modeled across microwave power levels of 1000 W, 1500 W, 2000 W, 2500 W, and 3000 W [8], with a measurement duration of 10 s. The gas flow input volumes of •OH and •O at different microwave powers are shown in Table 4.

Table 4

The volume of free radical gas stream input at various microwave power levels

Free radical airflow input volume	Microwave power [W]				
	1000	1500	2000	2500	3000
•OH, %	0.32	0.34	0.35	0.36	0.37
O, %	0.68	0.66	0.65	0.64	0.63
Flow rate, m/s	0.0579	0.0729	0.0879	0.1029	0.1179

Figure 7 illustrates that at 473 K and 3 m/s flue gas inlet velocity, the efficiency of toluene removal by •OH radicals increases with higher microwave reactor power. This adjustment alters the •OH radicals to toluene concentration ratio. Significant enhancement in toluene removal efficiency was observed when microwave power exceeded 2500 W, plateauing around 3000 W. At approximately 3000 W, gas uniformity within the pipeline improved. Considering practical industrial requirements and economic feasibility, microwave power levels for toluene removal should be carefully regulated, not exceeding 3000 W in actual production scenarios.

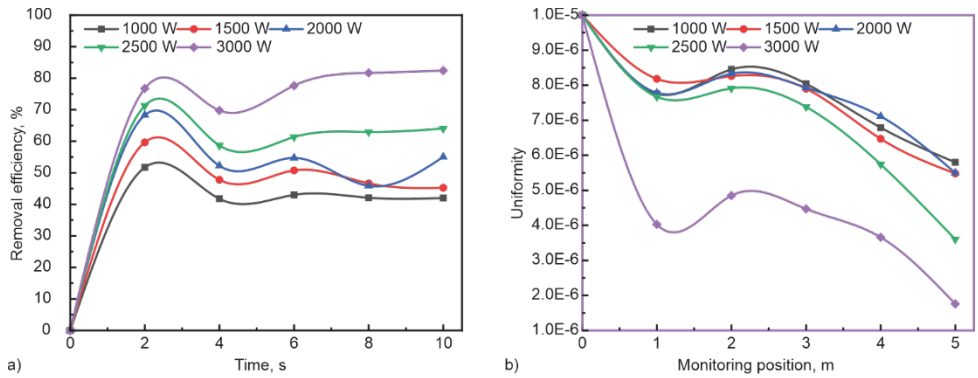

Fig. 7. Effect of microwave power at 473 K and gas velocity of 3 m/s on toluene removal efficiency (a) and homogeneity (b)

The microwave reactor operated at 3000 W with a flue gas inlet flow rate of 3 m/s. The temperature of the gas at the flue gas inlet was systematically adjusted in increments of 50 K from 373 K to 573 K to simulate pollutant removal within the pipeline. The influence of temperature variation on pollutant removal efficiency was examined over a measurement period of 10 s.

As shown in Fig. 8, the efficiency of toluene removal by ·OH radicals progressively increased with rising temperature. Minimal change in toluene removal efficiency was observed around 423 K, indicating a plateau in effectiveness. The most significant enhancement in toluene removal efficiency occurred at 523 K, reaching 97.83% removal efficiency within 5 meters of the pipeline. As temperatures continued to rise up to 573 K, further improvements in removal rate were marginal, suggesting saturation of removal efficiency. This demonstrates that temperature variation strongly influences the efficiency of pollutant removal.

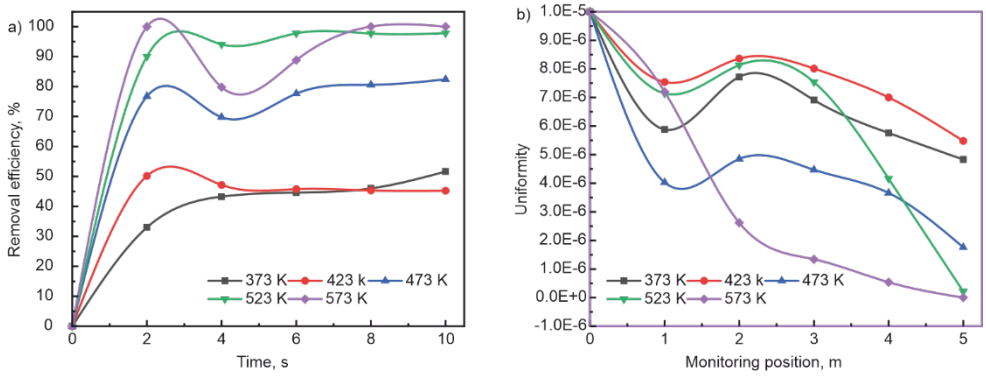

Fig. 8. Effect of temperature at a microwave power of 3000 W and 3 m/s gas velocity on toluene removal efficiency (a) and homogeneity (b)

The microwave reactor operated at 3000 W, with a flue gas inlet flow rate of 3 m/s and a temperature of 473 K. The moisture content of the flue gas inlet was systematically adjusted to simulate the removal efficiency of ·OH to toluene under varying moisture levels of 1, 3, 5, 7, and 9%. The impact of reactive moisture content on pollutant removal efficiency was examined over a measurement period of 10 s.

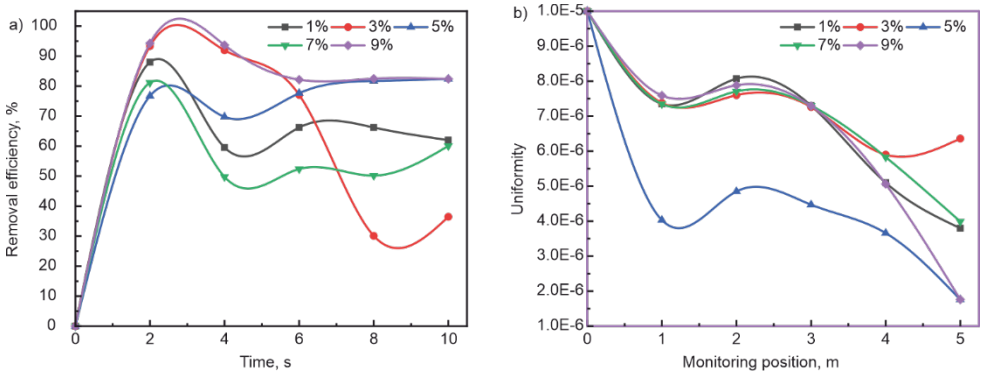

Fig. 9. Effect of moisture mass fraction at 473 K, a microwave power of 3000 W and gas velocity of 3 m/s on toluene removal efficiency (a) and homogeneity (b)

As illustrated in Fig. 9, the optimal toluene removal efficiency was observed at approximately 5% moisture content in the flue gas inlet. Both too low and too high moisture content were found to be detrimental to toluene degradation. Insufficient moisture led to a shortage of reactants involved in ·OH radical generation, thereby impeding toluene removal. Conversely, excessive moisture had a quenching effect on excited state radicals [24], resulting in reduced removal efficiency. Consequently, when the moisture content was at 3% and 7%, the removal efficiency decreased. Therefore, the most favorable removal efficiency and uniformity of toluene in the pipeline were achieved at around 5% moisture content.

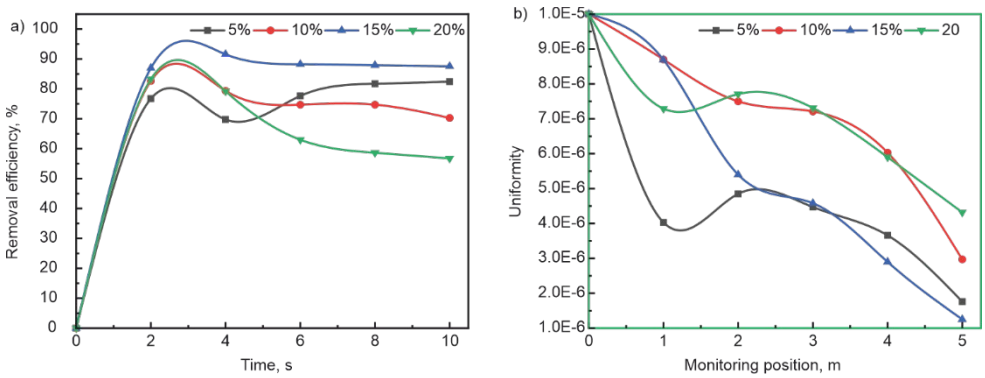

Fig. 10. Effect of oxygen mass fraction at 473 K, microwave power of 3000 W, and gas velocity of 3 m/s on toluene removal efficiency (a), and oxygen mass fraction on homogeneity (b)

The microwave reactor operated at 3000 W, with a flue gas inlet flow rate of 3 m/s and a temperature of 473 K. The oxygen content of the flue gas inlet was systematically varied to simulate the removal efficiency of ·OH from toluene under different oxygen levels of 5%, 10%, 15%, and 20%. The impact of reactive oxygen content on pollutant removal efficiency was examined over a measurement period of 10 s.

As depicted in Fig. 10, the efficiency of microwave and ·OH radical removal of flue gas improved as the oxygen content of the flue gas inlet increased from 5% to approximately 15%. Appropriately increasing the oxygen content was found to enhance the efficiency of toluene removal. However, when the oxygen content was raised to 20%, the removal reaction was somewhat inhibited. Therefore, maintaining the oxygen concentration of the flue gas as close as possible to around 15% is favorable for the toluene removal reaction. The microwave reactor operated at 3000 W, with a moisture content of 5%, an oxygen content of 5%, and a temperature of 473 K. The removal efficiency of ·OH from toluene under microwave irradiation was simulated across flue gas inlet flow rates of 1, 2, 3, 5, 8, and 10 m/s. The impact of reactive oxygen content on pollutant removal efficiency was investigated over a measurement period of 10 s. At slower flue gas inlet rates, the toluene did not reach the outlet within the 10-s measurement time. Hence, comparisons of toluene concentrations at different locations were made to analyze its removal.

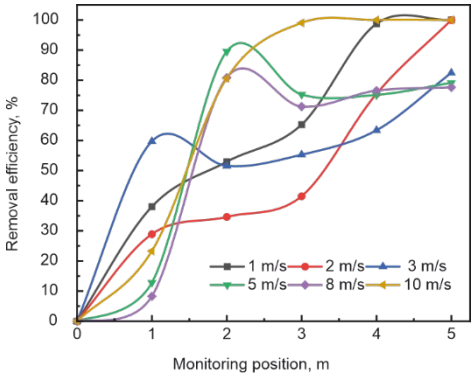

Fig. 11. Effect of flue gas inlet velocity at 473 K, microwave power of 3000 W, 5% O_2 content and 5% H_2O content on toluene removal efficiency (a) and homogeneity (b)

As depicted in Fig. 11, the removal efficiency of toluene at the outlet exhibited minimal variation when the flue gas inlet rate ranged from 3 to 8 m/s. Among the factors studied, the flue gas inlet rate had the least influence on toluene removal efficiency. Toluene was undetectable at the outlet when the flue gas inlet rates were 1 and 2 m/s, as it had not yet reached that point. The data at 3 m/s inlet rate provided valuable insights into toluene removal efficiency.

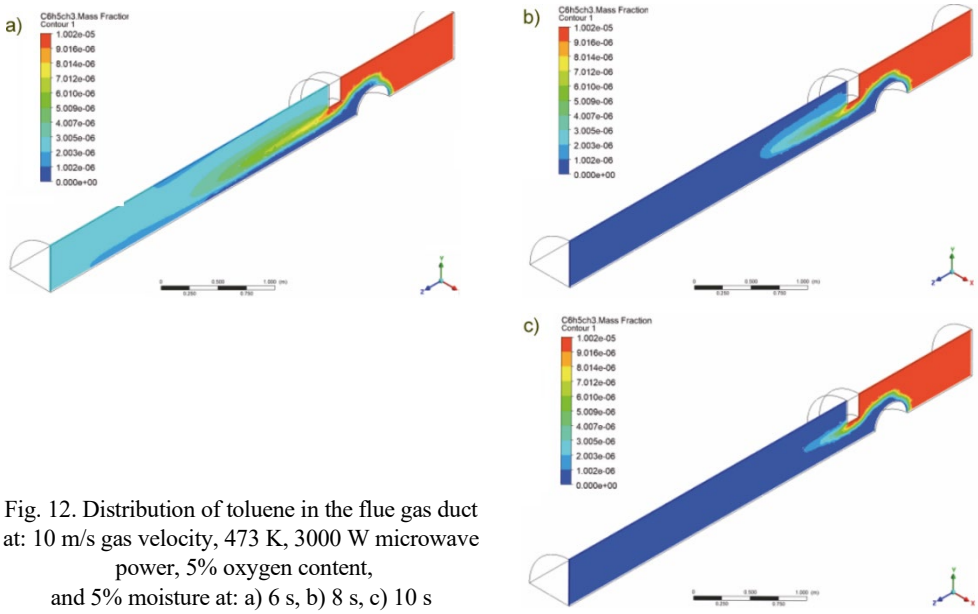

Fig. 12. Distribution of toluene in the flue gas duct at: 10 m/s gas velocity, 473 K, 3000 W microwave power, 5% oxygen content, and 5% moisture at: a) 6 s, b) 8 s, c) 10 s

At an inlet flue gas velocity of 10 m/s, the toluene concentration at the duct outlet was excessively low. Figure 12 illustrates that this is attributed to the high gas flow rate in the vicinity of the deflector plate, where the Reynolds number reaches approximately 3×10^5 in the subcritical region. This condition leads to gas recirculation and vortices behind the

deflector plate [25]. Consequently, toluene accumulates at the plate's rear end, resulting in undetectable levels at the exit of the flue gas pipeline. Thus, when employing this pipe model, it is advisable to maintain the flow velocity below 10 m/s. Alternatively, the addition of extra deflectors can be considered to alter the fluid flow direction.

The microwave reactor operated at 3000 W with a flue gas inlet flow rate of 3 m/s, 5% moisture, 5% oxygen content, and a temperature of 473 K. Removal efficiencies were simulated for toluene concentrations of 1 ppm, 10 ppm, 100 ppm, and 1000 ppm. It is noteworthy that the homogeneity at these concentrations was not assessed using the standard deviation of the gridded toluene concentration surface. Due to varying initial concentrations of toluene, the magnitude of standard deviation could not directly indicate homogeneity. The homogeneity was assessed as the quotient of the standard deviation across the inlet face and the initial toluene concentration.

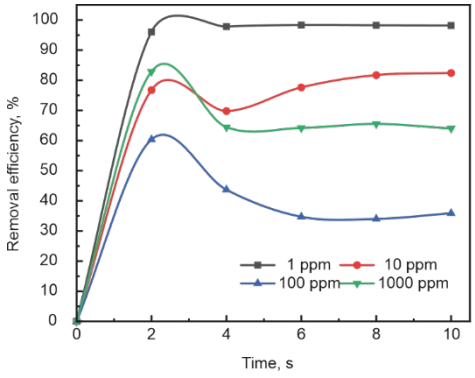

Fig. 13. Effect of toluene concentration on its removal efficiency at the gas velocity of 3 m/s, 473 K, 3000 W microwave power, 5% oxygen content and 5% moisture

As illustrated in Fig. 13, the toluene removal efficiency in the pipeline reached 98.17% when the toluene concentration was 1 ppm. However, as the initial toluene concentration increased, the removal efficiency gradually declined. Notably, concentrations exceeding 10 ppm resulted in a significant reduction in toluene removal efficiency.

3.3. BY-PRODUCT ANALYSIS

According to a previous study [8], there are solid, liquid, and gas phase products from the cracking of toluene during microwave discharge. Through gas chromatography (GC) detection and analysis, it was found that the gaseous product components were basically the same as those of conventional pyrolysis conditions, mainly two kinds of H_2 and CH_4, of which the volume percentage of H_2 was about 60%. By gas chromatography with mass spectrometry (GC-MS) detection and analysis, the liquid products of toluene cracking were enriched with a variety of PAH compounds, with the main components of phenanthrene ($C_{14}H_{10}$), 2,2-dimethylbiphenyl ($C_{14}H_{14}$), and biphenyl ($C_{12}H_{10}$), with volume percentages of 5.09, 4.86, and 3.48%, respectively. The solid phase products were examined

mainly using Fourier infrared spectroscopy (FTIR), XRD, SEM-EDS, and TEM. The results showed that the solid-phase products were carbon nanospheres with particle sizes smaller than 100 nm, irregular shapes, and a certain degree of graphitisation, and it was found that the particle size of the carbon spheres was smaller with the deepening of toluene cleavage.

The gas product had a high percentage of H_2 by volume (ca. 60%), which is environmentally friendly as a clean energy source whose combustion product is only water. However, H_2 is also a greenhouse gas, and increased concentrations in the atmosphere can still have an impact on the environment. CH_4 is a much more potent greenhouse gas, and its impact on global warming is much higher than that of CO_2 [26]. Therefore, emissions of methane need to be strictly controlled. It is worth noting that both major gas products have a high energy utilisation value, and thus both can be used for energy production by collecting them in an efficient manner, thus reducing pollution of the environment and dependence on traditional fossil fuels. The liquid products are mainly polycyclic aromatic hydrocarbon compounds (PAHs), a class of known carcinogens that pose a threat to human health and the environment [27]. Although the volume percentage of these compounds is low, their toxicity and bioaccumulation mean that even trace emissions need to be strictly controlled to prevent contamination of water bodies and soil. Nanocarbon spheres, a solid phase product, possess unique physicochemical properties and are potentially utilised in areas such as energy storage and catalyst carriers [28]. However, the small particle size of carbon nanospheres may migrate in the environment and affect the ecosystem. In addition, the discharge produces precipitated carbon with highly graphitised properties, which has some recycling value from the perspective of carbon material application.

3.4. APPLICATION POTENTIAL

The microwave discharge removal of VOCs (toluene) was numerically modelled to provide theoretical guidance for future research on VOC treatment technologies. With reference to the theoretical model of this study, a microwave discharge system for the removal of VOCs is designed for practical industrial applications, which mainly consists of a blower, dust collector, microwave generator, ducted reaction chamber, and by-product collection device. The VOCs enter the dust collector through the blower to remove solid particles, and the gas subsequently passes into the reaction chamber where it is subjected to microwave irradiation, and finally, other by-products, such as H_2, CH_4, are collected. Release in H_2O, CO_2 tail gas is environmentally friendly.

Since no catalyst is used, the system does not usually show significant changes in VOCs removal efficiency in long-term operation. In addition, the local temperature of the pipeline will increase significantly when subjected to long-term microwave irradiation, and the higher temperature is also conducive to the reaction, so high-temperature-resistant materials should be used in the construction of the pipeline system to avoid possible melting of the discharge area [29]. The microwave generator is the core of this system, and given

the need to be able to deliver sufficient microwave power to achieve effective removal of VOCs, the cost of this equipment depends on the power, efficiency, and durability of the microwave generator required for specific generation. The operating cost during system operation is mainly the microwave energy consumption per hour and the corresponding electricity cost. In addition, the energy consumption of high-power microwave discharge in industrial applications is controllable, while the heat generated during operation can be used to preheat the VOC gas, which is conducive to the long-term stable operation of the system [15]. The system, as a VOCs treatment technology, not only can obtain relevant policy benefits, but also the by-products (H_2, CH_4) obtained after toluene removal can be recovered and provide economic value. Based on the literature research and our simulation results, a cost analysis was carried out (the electricity price was 0.049 USD/kWh). The results are shown in Table 5. It is evident that microwave discharge technology has significant cost advantages, especially for the removal of high concentrations of VOCs.

Table 5

Cost analysis of VOCs treatment technology [USD/kg]

Technology	Low concentration (<1000 ppm）	High concentration (> 1000 ppm）
Plasma	0.67–1.22	0.0085–0.015
Biodegradation	1.89–3.66	0.85
Adsorption	1.28–1.40	0.13–0.18
Microwave discharge	1.03	0.00068

The microwave discharge technique offers several advantages over conventional control processes (Table 6).

Table 6

Performance and application scenarios of VOCs treatment technology [30]

Technique	Advantages	Disadvantages	Industrial applications
Adsorption	easy to operate, relatively low cost; can treat a wide range of VOCs	problems of secondary pollution; low treatment efficiency of high concentration VOCs	treatment of low concentration and large air volume VOCs, e.g., in the electronics industry, shoe-making industry, printing industry
Thermal oxidation	high treatment efficiency, completely decomposes VOCs; applicable to the treatment of high concentration VOCs	high energy consumption, high operating costs; high temperature required, high equipment material requirements; generation of nitrogen oxides and other by-products	treatment of high concentration VOCs in chemical and printing industries

Table 6

Performance and application scenarios of VOCs treatment technology [30]

Technique	Advantages	Disadvantages	Industrial applications
Membrane separation	lower energy consumption, flexible operating temperature, high selectivity of membrane materials, good separation effect	higher cost of the membrane materials, and easy to be contaminated and clogged; poor separation of mixed gases with complex components of VOCs	gas purification and recovery of VOCs in the petrochemical and food industries
Condensation	simple operation and relatively low investment in equipment	higher energy consumption, involving low temperature environment; low removal efficiency for low boiling point VOCs	handling of high boiling point, low concentration VOCs, e.g., certain solvent recovery
Microwave discharge	high treatment efficiency, rapidly decomposes VOCs; relatively low energy consumption, fast reaction speed; can be processed online without adding catalysts; able to treat a wide range of VOCs including compounds difficult to degrade	higher equipment and maintenance costs; higher requirements for equipment design and operation	suitable for applications requiring rapid treatment of VOCs, such as industrial exhaust gas purification

4. CONCLUSIONS

Microwave power and increased temperature are the factors primarily influencing toluene removal efficiency, with an increase in both parameters leading to a marked improvement in toluene removal efficiency. Specifically, at a microwave power of 3000 W and a temperature of 523 K, the toluene removal efficiency can reach 97.83%. Moisture and oxygen content, flue gas inlet rate, and toluene concentration have a secondary influence on toluene removal efficiency, with less impact compared to temperature and microwave power. The flue gas inlet rate exerts a significant effect on toluene removal efficiency. Although the inlet flow rate has little impact on toluene removal efficiency within the range of 1 m/s to 8 m/s, a flow rate of 10 m/s results in toluene reflux and vortex formation after the deflector plate. This accumulation of flue gas at the rear end of the deflector plate hinders the removal of toluene in the flue gas pipeline. Therefore, excessive flue gas inlet rates should be avoided.

ACKNOWLEDGEMENT

This research was supported by the Zhejiang Provincial Natural Science Foundation of China (Grant No. LTGS24E060005).

REFERENCES

[1] JIMENEZ J.L., CANAGARATNA M.R., DONAHUE N.M., PREVOT A.S.H., ZHANG Q., KROLL J.H., DECARLO P.F., ALLAN J.D., COE H., NG N.L., AIKEN A.C., DOCHERTY K.S., ULBRICH I.M., GRIESHOP A.P., ROBINSON A.L., DUPLISSY J., SMITH J.D., WILSON K.R., LANZ V.A., HUEGLIN C., SUN Y.L., TIAN J., LAAKSONEN A., RAATIKAINEN T., RAUTIAINEN J., VAATTOVAARA P., EHN M., KULMALA M., TOMLINSON J.M., COLLINS D.R., CUBISON M.J., E., DUNLEA J., HUFFMAN J.A., ONASCH T.B., ALFARRA M.R., WILLIAMS P.I., BOWER K., KONDO Y., SCHNEIDER J., DREWNICK F., BORRMANN S., WEIMER S., DEMERJIAN K., SALCEDO D., COTTRELL L., GRIFFIN R., TAKAMI A., MIYOSHI T., HATAKEYAMA S., SHIMONO A., SUN J.Y, ZHANG Y.M., DZEPINA K., KIMMEL J.R., SUEPER D., JAYNE J.T., HERNDON S.C., TRIMBORN A.M., WILLIAMS L.R., WOOD E.C., MIDDLEBROOK A.M., KOLB C.E., BALTENSPERGER U., WORSNOP D.R., *Evolution of organic aerosols in the atmosphere*, Science, 2009, 326, 1525–1529. DOI: 10.1126/science.1180353.

[2] UTEMBE S.R., WATSON L.A., SHALLCROSS D.E., JENKIN M.E., *A common representative intermediates (CRI) mechanism for VOC degradation. Part 3: Development of a secondary organic aerosol module*, Atm. Environ., 2009, 43, 1982–1990. DOI: 10.1016/j.atmosenv.2009.01.008.

[3] ZHANG X., GAO B., ELISE C.A., CAO C., LI Y., *Adsorption of VOCs onto engineered carbon materials: A review*, J. Hazard. Mater., 2017, 338, 102–123. DOI: 10.1016/j.jhazmat.2017.05.013.

[4] MA Y., CHEN N., *Treatment of tar processing exhaust gases with regenerative combustion ovens*, Fuel Chemi. Proc., 2018, 2, 51–53 + 58.

[5] FUTAMURA S., ZHANG A., EINAGA H., KABASHIMA H., *Involvement of catalyst materials in nonthermal plasma chemical processing of hazardous air pollutants*, Catal. Today, 2002, 72, 259–265. DOI: 10.1016 /S0920-5861(01)00503-X.

[6] KIM H., OH S., OGATA A., FUTAMURA S., *Decomposition of gas-phase benzene using plasma-driven catalyst (PDC) reactor packed with Ag/TiO_2 catalyst*, Appl. Catal. B Environ., 2005, 56, 213–220. DOI: 10.1016/j.apcatb.2004.09.008.

[7] KAMAL M.S., RAZZAK S.A., HOSSAIN M.M., *Catalytic oxidation of volatile organic compounds (VOCs). A review*, Atmos. Environ., 2016, 140, 117–134. DOI: 10.1016/j.atmosenv.2016.05.031.

[8] ZHOU Y., *Experimental and mechanical study of microwave induced metal discharge enhanced biomass tar cracking*, Shandong University, Jinan 2019. DOI: 10.7666/d.Y3517605.

[9] GUO T., LI X., LI J., PENG Z., XU L., DONG J., PING C., ZHOU Z., *On-line quantification and human health risk assessment of organic by-products from the removal of toluene in air using non-thermal plasma*, Chemosphere, 2018, 194, 139–146. DOI: 10.1016/j.chemosphere.2017.11.173.

[10] ATKINSON R., AREY J., *Atmospheric degradation of volatile organic compounds*, Chem. Rev., 2003, 103, 4605–4638. DOI: 10.1021/cr0206420.

[11] SHEN X., ZHAO Y., CHEN Z., HUANG D., *Heterogeneous reactions of volatile organic compounds in the atmosphere*, Atmos. Environ., 2013, 68, 297–314. DOI: 10.1016/j.atmosenv.2012.11.027.

[12] CHENG S., ZHAO Y., ZHANG J., ZHANG J., *Multi-physical field simulation technology and software development status of power equipment*, Power Syst. Autom., 2022, 46, 121–137. DOI: 10.7500/AEPS2022 0506002.

[13] WANG B., *Development of computational fluid dynamics and applied research*, South. Agric. Mach., 2018, 49, 145. DOI: 10.3969/j.issn.1672-3872.2018.09.113.

[14] MOUSAVI S.M., FATEHI H., BAI X., *Numerical study of the combustion and application of SNCR for NO_x reduction in a lab-scale biomass boiler*, Fuel, 2021, 293, 120154. DOI: 10.1016/j.fuel.2021.120154.

[15] FENG Y., WANG W., WANG Y., SUN J., ZHANG C., SHAHZAD Q., MAO Y., ZHAO X., SONG Z., *Experimental study of destruction of acetone in exhaust gas using microwave-induced metal discharge*, Sci. Total Environ., 2018, 645, 788–795. DOI: 10.1016/j.scitotenv.2018.07.183.

[16] WANG Y., CHEN W., ZHOU Y., ZHONG Y., ZHONG N., JIA S., HUANG K., *Investigation of microwave enhanced catalytic degradation of VOCs with a novel double ridge field compressed cavity*, Chem. Eng. J., 2022, 442, 136181. DOI: 10.1016/j.cej.2022.136181.

[17] LI Z., LIU J., GAO B., BO L., *Cu-Mn-CeO_x loaded ceramic catalyst for non-thermal sterilization and microwave thermal catalysis of VOCs degradation*, Chem. Eng. J., 2022, 442, 136288. DOI: 10.1016/j.cej.2022.136288.
[18] SU T., DENG S., LI F., *Monte Carlo simulation of chemical reaction kinetics in Matlab environment*, J. Guangdong Institute of Technology, 2012, 33, 1–3.
[19] LI J., LIN H., ZHAO W., CHEN G., *Instant modification of graphite nanosheets by the grafting of a styrene oligomer under microwave radiation*, J. Appl. Polym. Sci., 2008, 109, 1377–1380. DOI: 10.1002/app.28101.
[20] WEN Z., LIU Y., SHEN H., LI Y., XU J., *A theoretical study on the destruction of typical biomass tar components (toluene, phenol and naphthalene) by OH radical*, J. Indian Chem. Soc., 2021, 98, 100015. DOI: 10.1016/j.jics.2021.100015.
[21] QIU R., *Research on microwave plasma chemical vapour deposition system*, University of Electronic Science and Technology of China, Chengdu 2012. DOI: 10.7666/d.D818359.
[22] CHANG M.B., BALBACH J.H., ROOD M.J., KUSHNER M.J., *Removal of SO_2 from gas streams using a dielectric barrier discharge and combined plasma photolysis*, J. Appl. Phys., 1991, 69, 4409–4417. DOI: 10.1063/1.348367.
[23] WU Z., *Study on the mechanism of removal of multiple pollutants from flue gas by direct current corona discharge radical cluster*, Zhejiang University, Hangzhou 2006.
[24] HE G., CHEN C., YANG J., JIAN H., XU G., *Proof of selective triplet state quenching in the theory of chemically induced dynamically electronically polarised radical-triplet pairs*, Chinese J. Magn. Res., 1998, 3, 197–203.
[25] HAO Z., LI W., FANG Q., LI L., *Simulation calculation of cylindrical winding at different Reynolds numbers*, J. Wuhan University of Technology, 2008, 30, 129–132. DOI: 10.3963/j.issn.1671-4431.2008.12.033.
[26] PARK J., ATTIA N.F., JUNG M., LEE M.E., LEE K., CHUNG J., OH H., *Sustainable nanoporous carbon for CO_2, CH_4, N_2, H_2 adsorption and CO_2/CH_4 and CO_2/N_2 separation*, Energy, 2018, 158, 9–16. DOI: 10.1016/j.energy.2018.06.010.
[27] AL-HARBI M., AL-ENZI E., AL-MUTAIRI H., WHALEN J.K., *Human health risks from brominated flame retardants and polycyclic aromatic hydrocarbons in indoor dust*, Chemosphere, 2021, 282, 131005. DOI: 10.1016/j.chemosphere.2021.131005.
[28] RODRIGUEZ-NARVAEZ O.M., PERALTA-HERNANDEZ J.M., GOONETILLEKE A., BANDALA E.R., *Biochar-supported nanomaterials for environmental applications*, J. Ind. Eng. Chem., 2019, 78, 21–33. DOI: 10.1016/j.jiec.2019.06.008.
[29] WANG W., LIU Z., SUN J., MA Q., MA C., ZHANG Y., *Experimental study on the heating effects of microwave discharge caused by metals*, AIChE J., 2012, 58, 3852–3857. DOI: 10.1002/aic.13766.
[30] LIU R., WU H., SHI J., XU X., ZHAO D., NG Y.H., ZHANG M., LIU S., DING H., *Recent progress on catalysts for catalytic oxidation of volatile organic compounds: a review*, Catal. Sci. Technol., 2022, 12, 6945–6991. DOI: 10.1039/D2CY01181F.